



Supporting Information

An Atomic Insight into the Chemical Origin and Variation of the Dielectric Constant in Liquid Electrolytes

Nan Yao, Xiang Chen,* Xin Shen, Rui Zhang, Zhong-Heng Fu, Xia-Xia Ma, Xue-Qiang Zhang,
Bo-Quan Li, and Qiang Zhang*

anie_202107657_sm_miscellaneous_information.pdf

SUPPORTING INFORMATION

Experimental Procedures

1.1. Molecular dynamics (MD) simulations

MD simulations were performed using the Large Scale Atomic/Molecular Massively Parallel Simulator (LAMMPS) code.^[1] Pure organic solvent systems were all composed of 200 solvent molecules. Solvent mixture systems contained 400 molecules in total with each component occupying a certain number of molecules according to the ratios. Constructed models of electrolytes with salts and diluents are listed in Table S3–5. Parameters for organic solvents were generated by LigParGen web server while the parameters for Li⁺, PF₆⁻, and FSI⁻ were obtained from Jensen *et al.*, Doherty *et al.*, and Lopes *et al.*, respectively.^[2] The initial atomic coordinates were generated with Packing Optimization for Molecular Dynamics Simulations (Packmol) program.^[3]

The periodic boundary conditions (PBCs) were applied in all three directions for all simulations. A cutoff of 12 Å was used for both van der Waals interactions and long-range correction (particle–particle particle-mesh) of Coulombic interactions. The time step was fixed to be 1 fs. Pure organic solvent systems were first equilibrated in NPT ensemble using the Parrinello–Rahman barostat for 3 ns to maintain a temperature of 298 K (and other temperatures for temperature dependence investigation) and a pressure of 1 atm with time constants of 0.1 and 1 ps, respectively.^[4] Other systems were first equilibrated in NPT ensemble for 0.5 ns and then heated from 298 to 350 K for 0.5 ns, and maintained at 350 K for 1 ns. Subsequently, the models were annealed from 350 to 298 K in 0.5 ns and equilibrated at 298 K in NPT ensemble for another 1 ns. A period no shorter than 20 ns were finally conducted for all systems in NVT ensemble under Nose–Hoover thermostat.^[5] The dipole moment of the system was output every 1000 steps during NVT simulations and used for calculation of dielectric constant.

1.2. Calculation of dielectric constant

The dielectric constant of liquid electrolytes is calculated according to formula S1:^[6]

$$\varepsilon = 1 + \frac{\langle M^2 \rangle - \langle M \rangle^2}{3\varepsilon_0 V k_B T} \quad (\text{S1})$$

where ε is the dielectric constant of specific system, ε_0 the dielectric constant of vacuum, V the volume of the simulation box, k_B the Boltzmann constant, T the temperature. $M = \sum \vec{\mu} = \sum q\vec{r}$ is the total dipole moment of the system where q and \vec{r} are the charge and position of atoms, respectively.

Total dipole moment of the system (M in formula S1) and square of it (M^2) were both averaged over 18000 frames, which means the dielectric constant is calculated from 18 ns to the end of NVT production run. For systems with salts, only the dipole moment of contact ion pairs (CIP) was included into the system dipole moment, since large aggregates have negligible dipole moments and thus have little influence on the dielectric constant of the electrolyte.^[7]

1.3. Density functional theory (DFT) calculations

The CM5 (Charge Model 5) charge, ESP (Electrostatic Potential) charge, dipole moments of solvents, and binding energy between solvent molecules or Li⁺ and anions (E_b , defined as formula S2 where M and N can be solvent, Li⁺, or anion) were all computed by DFT calculations, which were performed in Gaussian (G09) program.^[8] Becke's three-parameter hybrid method using the Lee–Yang–Parr correlation functional (B3LYP) and 6-311++G(d, p) basis set were chosen.^[9] The solvation effect was considered by SMD model.^[10] The CM5 charge in gas phase was directly obtained by Hirshfeld population analysis in G09 while both gas- and liquid-phase ESP charges were obtained according to the Merz-Singh-Kollman scheme.^[11] RESP charges were calculated based on ESP charges using Multiwfn program.^[12]

$$E_b = E_{M+N} - E_M - E_N \quad (\text{S2})$$

1.4. Machine learning

The artificial neural network (ANN) model was implemented TensorFlow and trained using gradient descent optimizer with a learning rate of 0.1.^[13] The ANN model includes an input layer, a hidden layer, and an output layer, which are consisted of two, six, and one nodes, respectively. Only activation function of ReLU was adopted in the hidden layer. The loss function is defined as the mean square error between the predicted and real natural logarithm of dielectric constant. Twenty-thousand step training was conducted and the final loss function was smaller than 0.01.

SUPPORTING INFORMATION

Supporting Figures

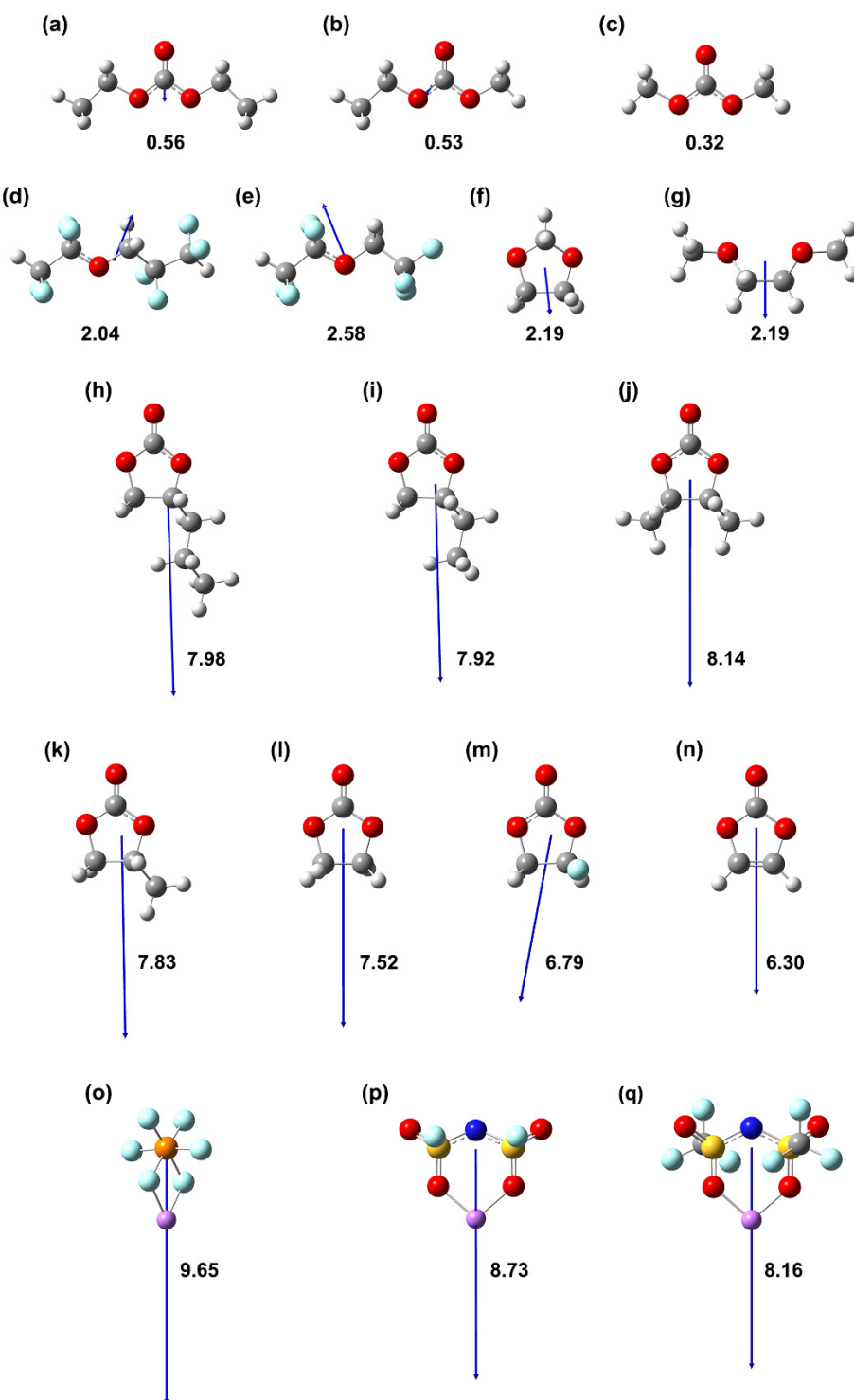


Figure S1. Molecular structures and dipole moments of the solvents and salts. (a) DEC, (b) EMC, (c) DMC, (d) HFE, (e) TFETFE, (f) DOL, (g) DME, (h) PIC, (i) BC, (j) BC23, (k) PC, (l) EC, (m) FEC, (n) VC, (o) LiPF₆, (p) LiFSI, and (q) LiTFSI. White, purple, grey, blue, red, cyan, orange, and yellow balls represent H, Li, C, N, O, F, P, and S atoms respectively. Below each molecular structure is the corresponding dipole moment (unit: Debye) of solvents and salts.

SUPPORTING INFORMATION

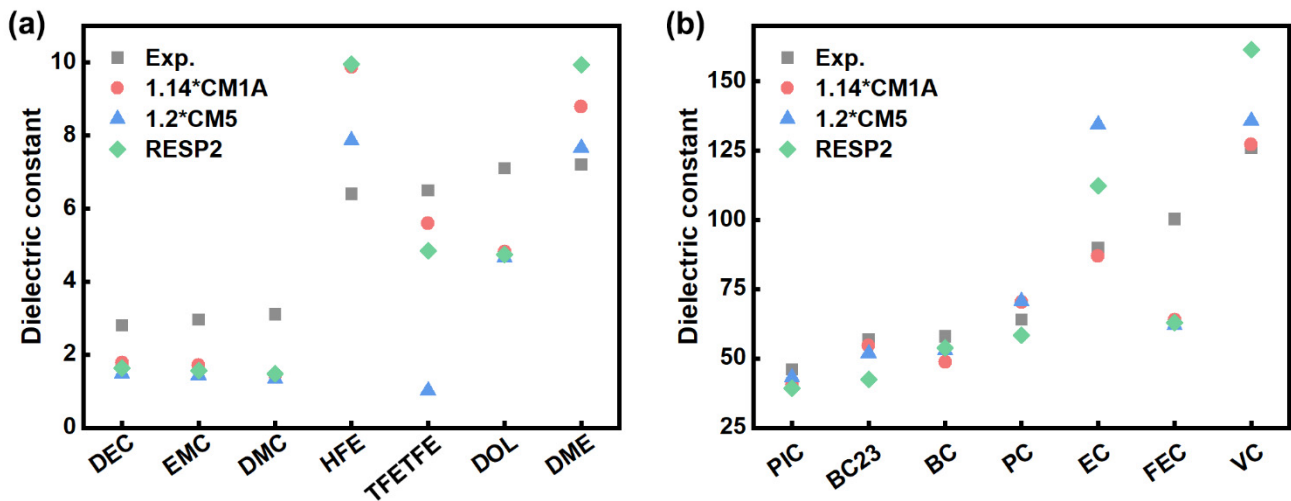


Figure S2. Dielectric constant of pure organic solvents calculated by three different charge models at 298 K (EC at 315 K). (a) Dielectric constant of DEC, EMC, DMC, HFE, TFETFE, DOL, and DME, which have relatively small dielectric constant. (b) Dielectric constant of PIC, BC, BC23, PC, EC, FEC, and VC, which have relatively large dielectric constant.

SUPPORTING INFORMATION

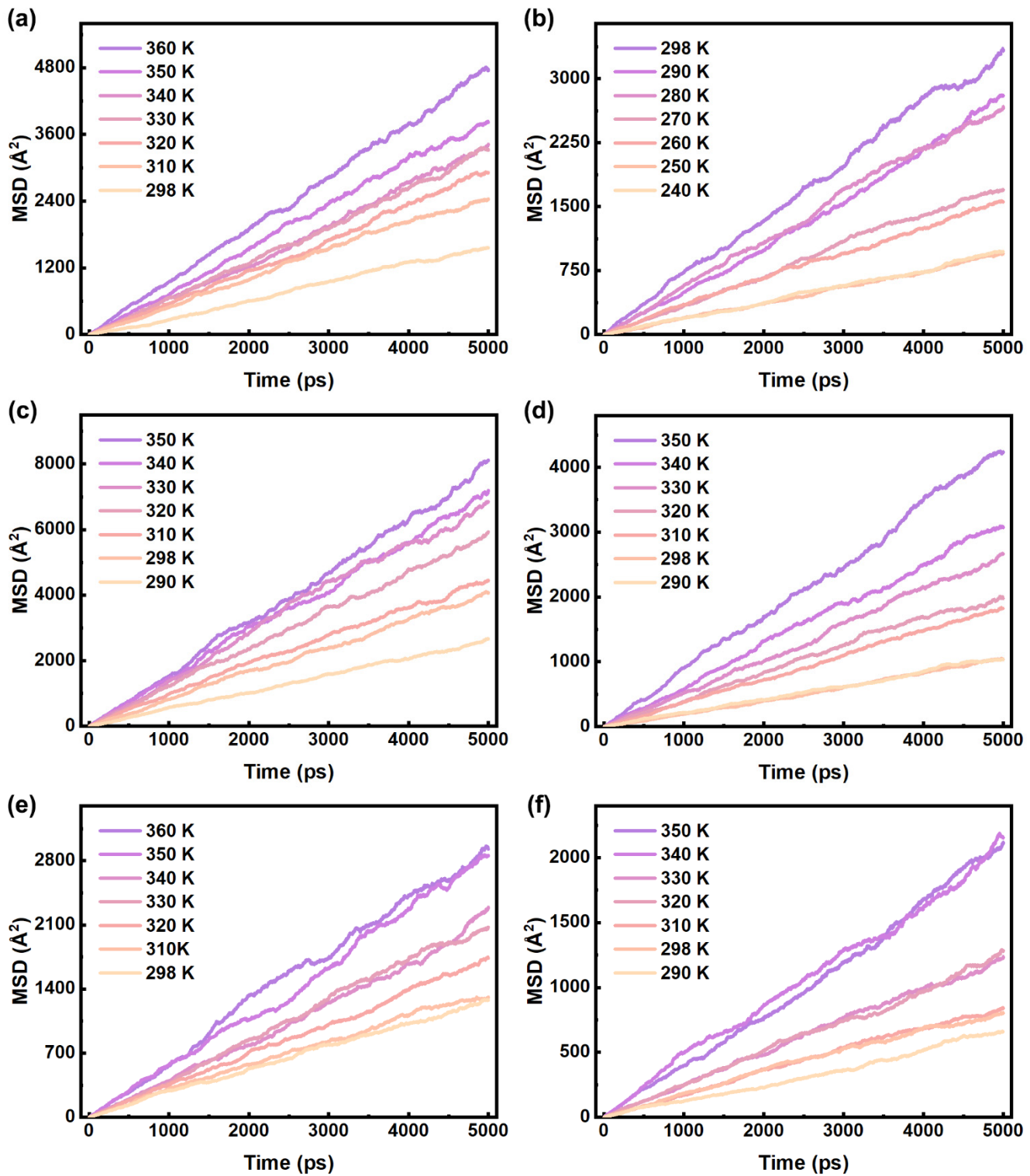


Figure S3. The mean square displacement (MSD) of different solvent systems at different temperatures: (a) DMC, (b) TFETFE, (c) DME, (d) HFE, (e) FEC, and (f) PC.

SUPPORTING INFORMATION

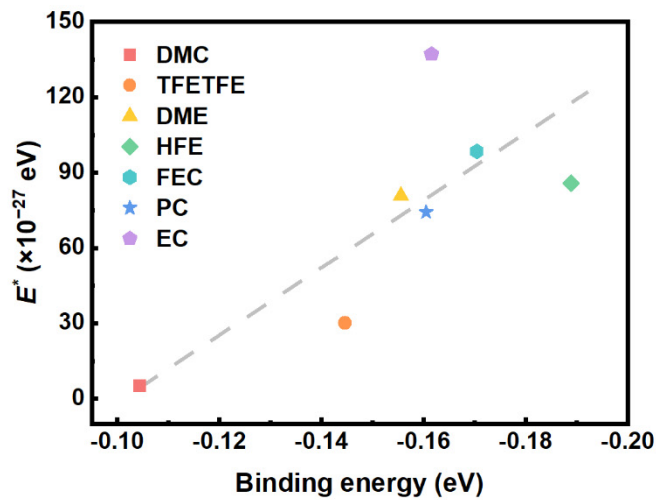
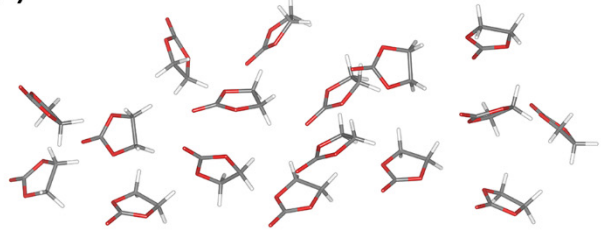


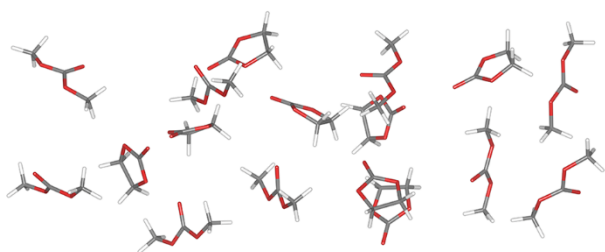
Figure S4. The relationship between strength of intermolecular interactions and E^* (energy barrier of overcoming interactions between molecules).

SUPPORTING INFORMATION

(a)



(b)



(c)

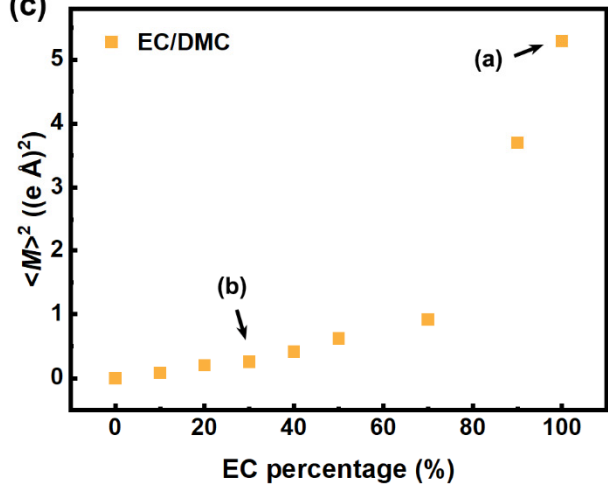


Figure S5. MD simulation snapshots of (a) EC at 298 K and (b) EC/DMC mixtures with a molar ratio of 3:7. (c) The square of the average total dipole moment ($\langle M \rangle^2$) of EC/DMC mixtures at different EC percentages.

SUPPORTING INFORMATION

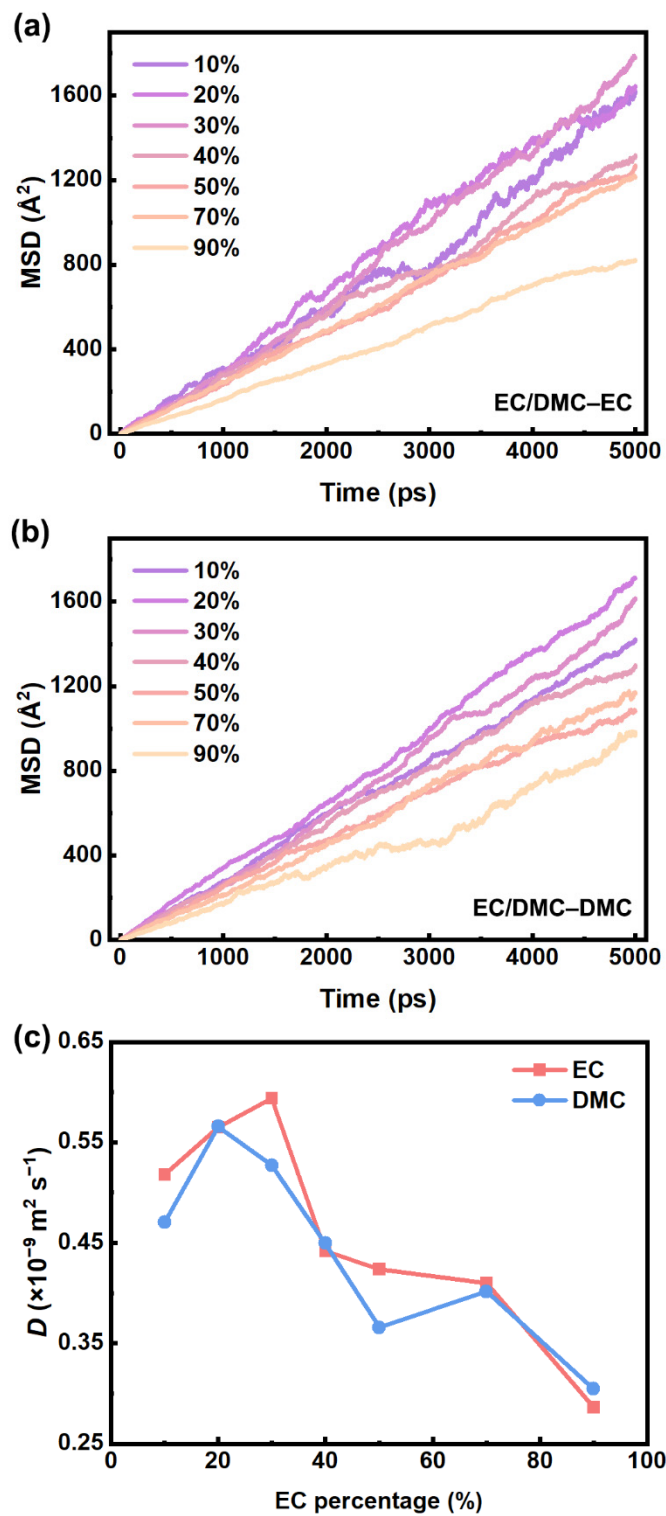


Figure S6. The MSD and diffusion coefficient of EC/DMC binary mixtures. The MSD of (a) EC and (b) DMC at different EC percentages. (c) The diffusion coefficients of EC and DMC at different EC percentages.

SUPPORTING INFORMATION

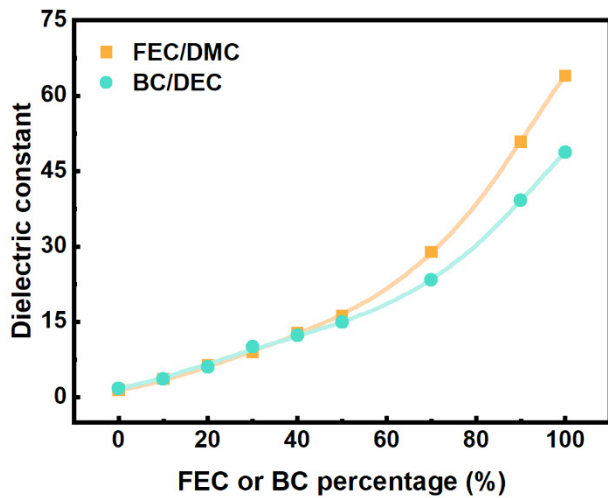
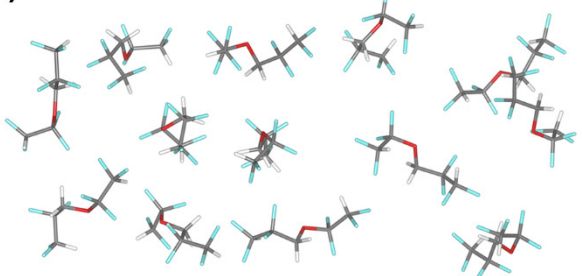


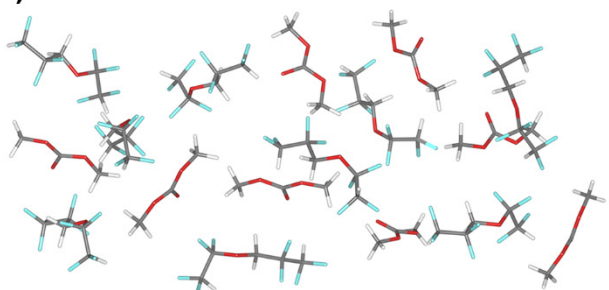
Figure S7. Dielectric constant of FEC/DMC and BC/EMC mixed solvents and the corresponding fitting curves.

SUPPORTING INFORMATION

(a)



(b)



(c)

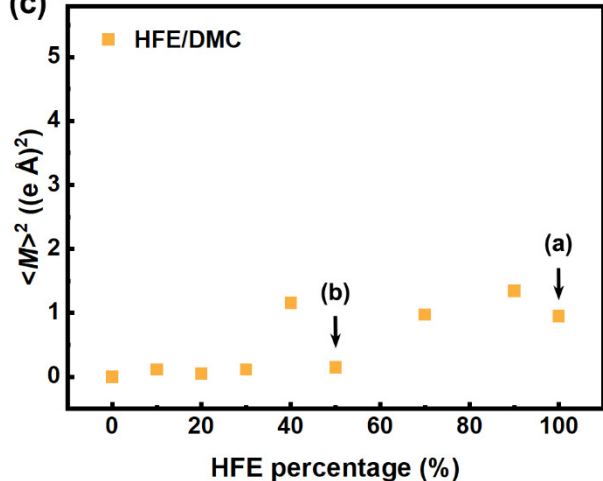


Figure S8. MD simulation snapshots of (a) HFE at 298 K, (b) HFE/DMC mixtures with a molar ratio of 5:5, (c) DME at 298 K, and (d) DME/DOL mixtures with a molar ratio of 5:5. (c) The square of the average total dipole moment ($\langle M \rangle^2$) of HFE/DMC mixtures at different HFE molar percentage.

SUPPORTING INFORMATION

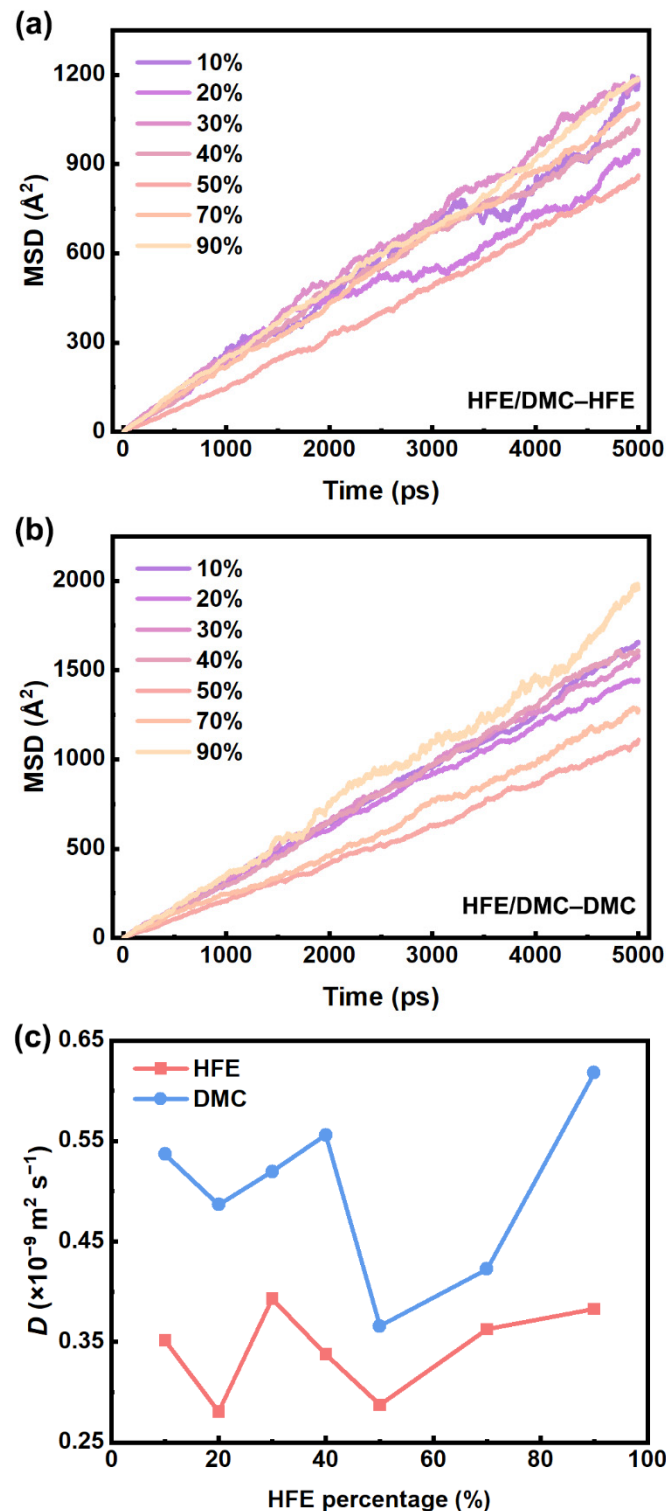


Figure S9. The MSD and diffusion coefficient of HFE/DMC binary mixtures. The MSD of (a) HFE and (b) DMC at different HFE percentages. (c) The diffusion coefficients of HFE and DMC at different HFE percentages.

SUPPORTING INFORMATION

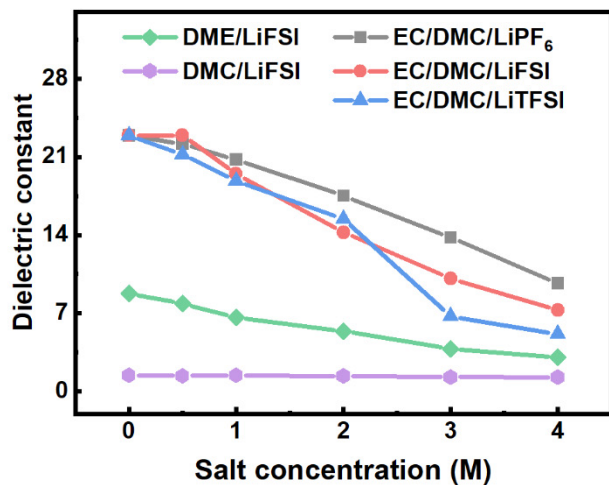


Figure S10. The dielectric constant of solvents in corresponding electrolytes.

SUPPORTING INFORMATION

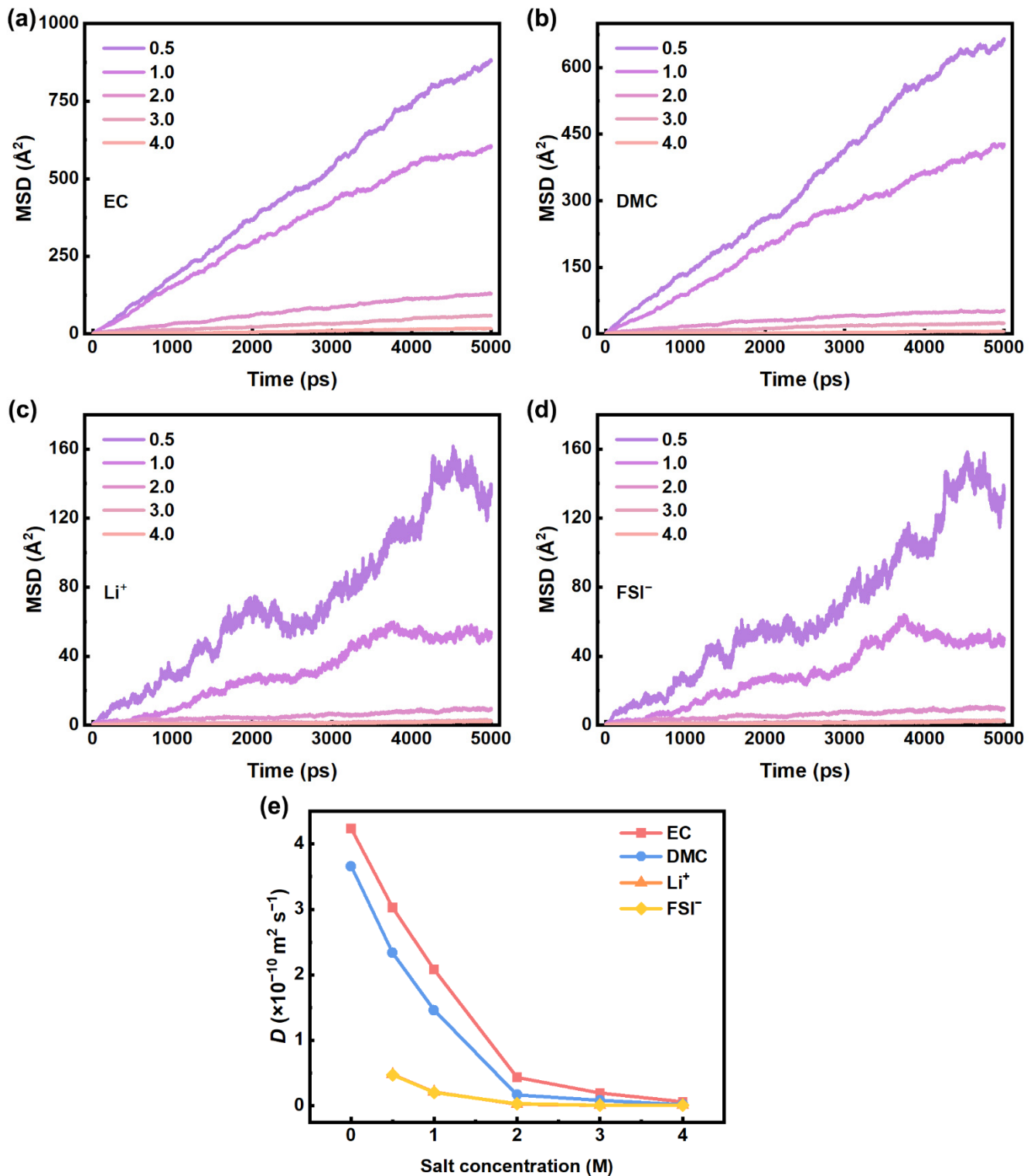


Figure S11. The MSD and diffusion coefficient of EC/DMC/LiFSI at different LiFSI concentrations (EC and DMC with a molar ratio of 1:1). The MSD of (a) EC, (b) DMC, (c) Li^+ , and (d) FSI^- . (e) The diffusion coefficients of EC, DMC, Li^+ , and FSI^- .

SUPPORTING INFORMATION

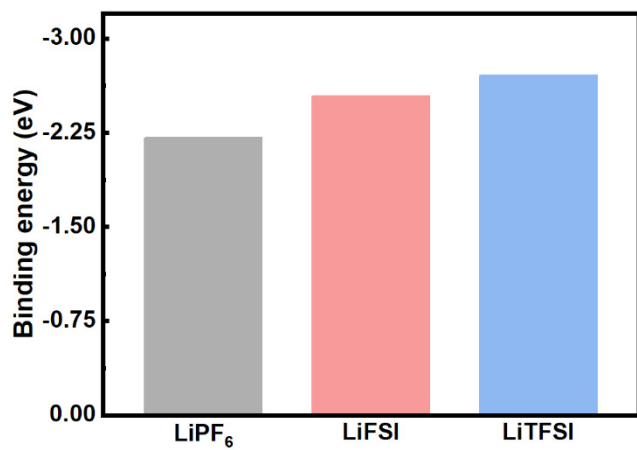


Figure S12. The binding energy between Li^+ - PF_6^- , Li^+ - FSI^- , and Li^+ - TFSI^- .

SUPPORTING INFORMATION

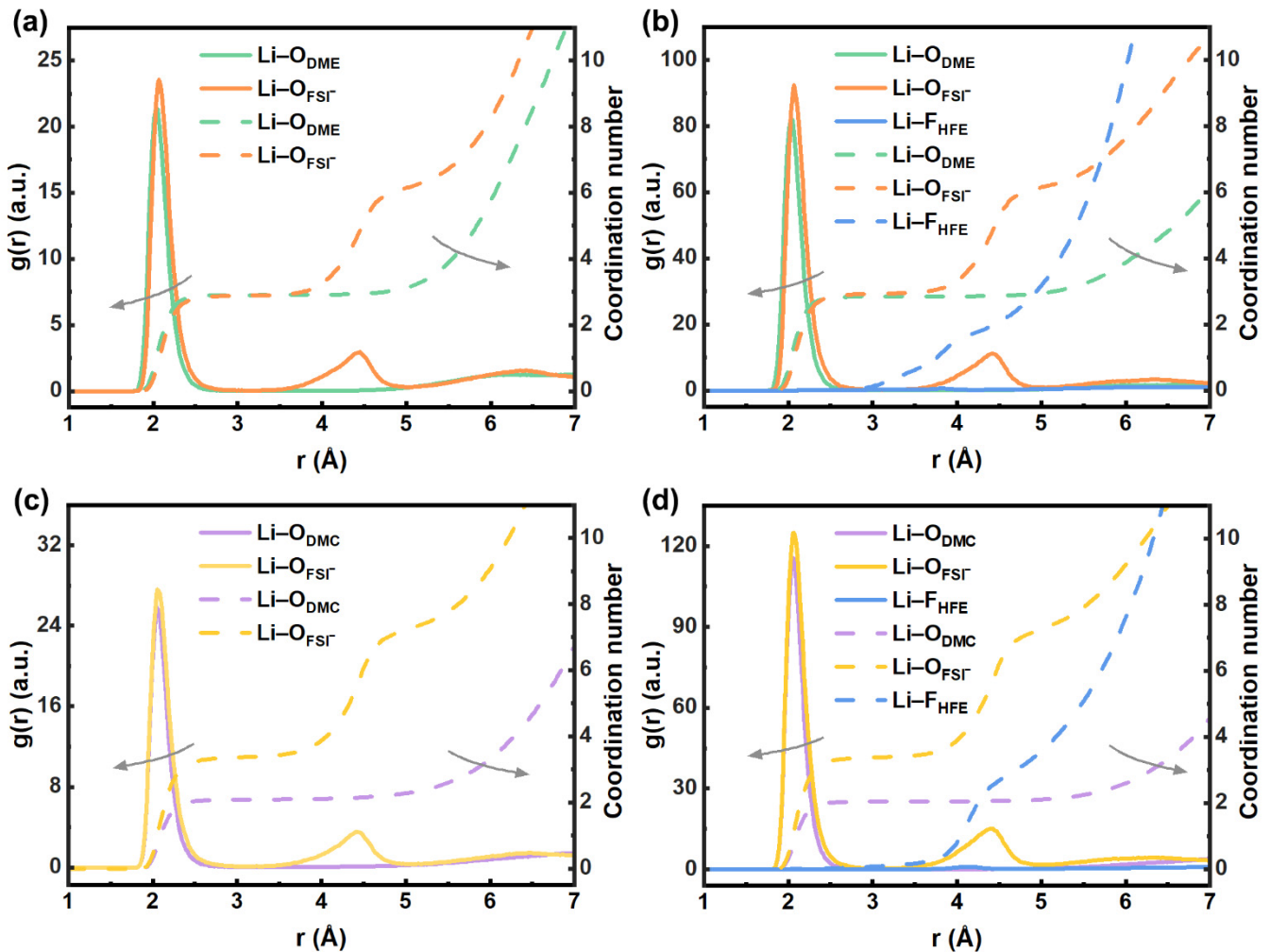


Figure S13. Radial distribution function of $\text{Li}-\text{O}$ (oxygen atoms of solvents or salts) and coordination number around Li^+ in (a) 4.0 M DME/LiFSI, (b) 4.0 M DME/HFE/LiFSI, (c) 4.0 M DMC/LiFSI, and (d) 4.0 M DMC/HFE/LiFSI (“4.0 M” in electrolytes with diluents means the electrolyte concentration is 4.0 M before the addition of diluents).

SUPPORTING INFORMATION

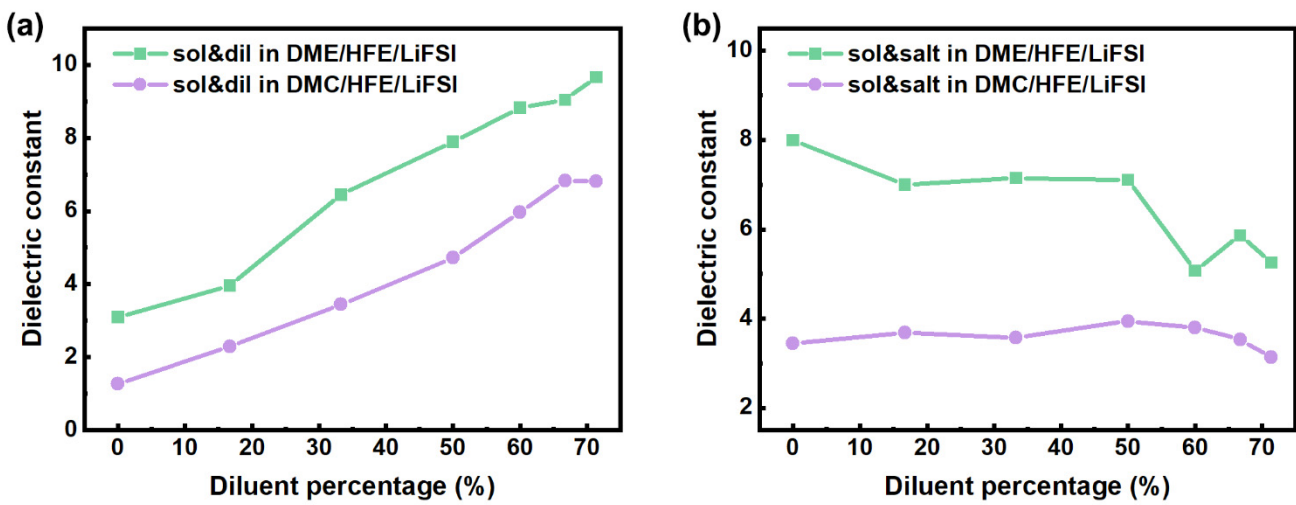


Figure S14. The dielectric constant of (a) solvents/diluents and (b) solvents/salts in 4.0 M DME/HFE/LiFSI and 4.0 M DMC/HFE/LiFSI.

SUPPORTING INFORMATION

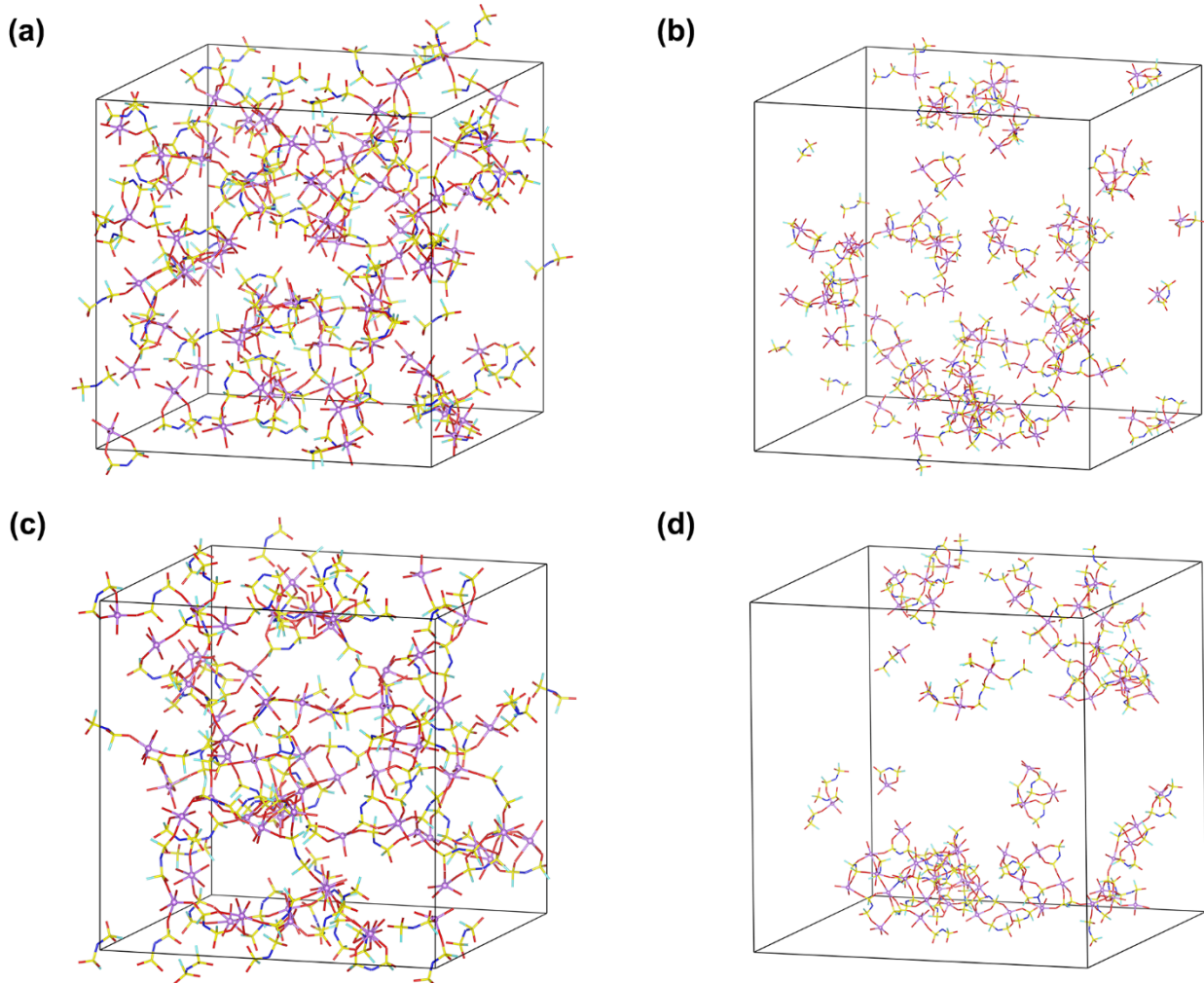


Figure S15. MD simulation snapshots of (a) 4.0 M DME/LiFSI, (b) 4.0 M DME/HFE/LiFSI, (c) 4.0 M DMC/LiFSI, and (d) 4.0 M DMC/HFE/LiFSI. Purple, blue, red, light blue, and yellow represent Li, N, O, F, and S atoms respectively. Only Li^+ , FSI^- , and the first coordinated atom of Li^+ are shown for clarity.

SUPPORTING INFORMATION

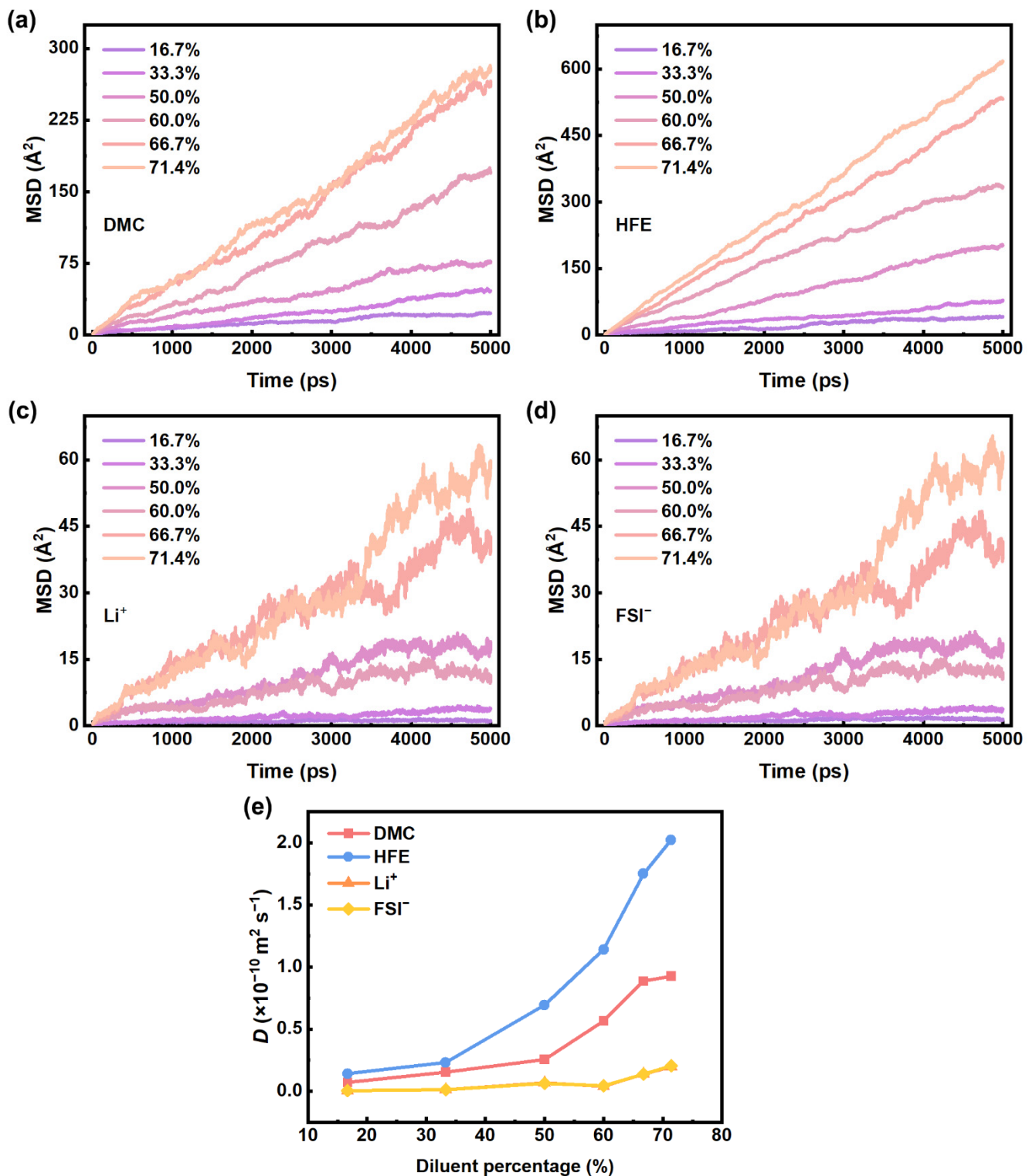


Figure S16. The MSD and diffusion coefficient of 4.0 M DMC/HFE/LiFSI at different diluent percentages (“4.0 M” means the electrolyte concentration is 4.0 M before the addition of diluents). The MSD of (a) DMC, (b) HFE, (c) Li⁺, and (d) FSI⁻. (e) The diffusion coefficients of DMC, HFE, Li⁺, and FSI⁻.

SUPPORTING INFORMATION

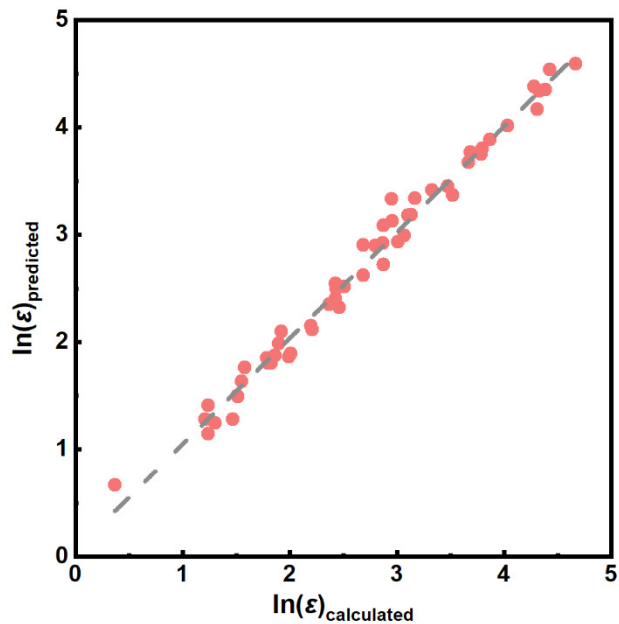


Figure S17. Comparison of the dielectric constant of EC/DMC/LiFSI predicted from machine-learning with those calculated by MD simulations.

SUPPORTING INFORMATION**Supporting Tables****Table S1.** Fitting parameters A and E^* in formula 1 for description of dielectric constant dependence on temperature.

Solvent	A	$E^* (\times 10^{-27} \text{ eV})$	R^2
DMC	1.3	5.2	0.9336
TFETFE	2.8	30.2	0.9066
DME	1.4	80.7	0.9561
HFE	1.3	85.8	0.9767
FEC	6.4	98.5	0.9488
PC	12.2	74.4	0.9393
EC	4.7	137.0	0.9766

SUPPORTING INFORMATION

Table S2. Fitting parameters $m_i (i = 0, 1, 2)$ in formula 3 for description of dielectric constant of solvent mixtures.

Solvent	m_0	m_1	m_2	R^2
EC/DMC	2.3	-3.0	2.6	0.9999
PC/EMC	2.4	-2.5	0.8	0.9995
FEC/DMC	2.2	-2.2	2.1	0.9999
BC/DEC	1.9	-2.5	2.1	0.9995

SUPPORTING INFORMATION

Table S3. The number and corresponding concentration of high-concentration electrolyte components in MD simulation models.

Model	Solvent 1	Solvent 2	Salt
EC/DMC/LiPF ₆			15 (0.5 M), 30 (1.0 M),
EC/DMC/LiFSI	200	200	61 (2.0 M), 91 (3.0 M),
EC/DMC/LiTFSI			121 (4.0 M)
DME/LiFSI	200		10 (0.5 M), 21 (1.0 M), 42 (2.0 M), 63 (3.0 M), 84 (4.0 M)
DMC/LiFSI	200		8 (0.5 M), 17 (1.0 M), 34 (2.0 M), 51 (3.0 M), 68 (4.0 M)

SUPPORTING INFORMATION**Table S4.** The number and corresponding percentage of localized high-concentration electrolyte components in MD simulation models.

Model	Solvent	Salt	Diluent
4.0 M DME/HFE/LiFSI	200	84	0 (16.7%), 100 (33.3%), 200 (50.0%), 300 (60.0%), 400 (66.7%), 500 (71.4%)
4.0 M DMC/HFE/LiFSI	200	68	

SUPPORTING INFORMATION

Table S5. The number of EC, DMC, and LiFSI in MD simulation models with different EC molar percentages and salt concentrations.

Model	EC	DMC	LiFSI
EC/DMC/LiFSI	40	360	17 (0.5 M), 33 (1.0 M), 66 (2.0 M), 100 (3.0 M), 133 (4.0 M)
	80	320	16 (0.5 M), 32 (1.0 M), 65 (2.0 M), 97 (3.0 M), 130 (4.0 M)
	120	280	16 (0.5 M), 32 (1.0 M), 63 (2.0 M), 95 (3.0 M), 127 (4.0 M)
	160	240	16 (0.5 M), 31 (1.0 M), 62 (2.0 M), 93 (3.0 M), 127 (4.0 M)
	200	200	15 (0.5 M), 30 (1.0 M), 61 (2.0 M), 91 (3.0 M), 121 (4.0 M)
	280	120	14 (0.5 M), 29 (1.0 M), 58 (2.0 M), 87 (3.0 M), 115 (4.0 M)
	360	40	14 (0.5 M), 27 (1.0 M), 55 (2.0 M), 82 (3.0 M), 110 (4.0 M)

SUPPORTING INFORMATION

References

- [1] P. Steve, *J. Comput. Phys.* **1995**, *117*, 1–19.
- [2] a) L. S. Dodd, I. C. de Vaca, J. Tirado-Rives, W. L. Jorgensen, *Nucleic Acids Res.* **2017**, *45*, W331–W336; b) B. Doherty, X. Zhong, S. Gathiaka, B. Li, O. Acevedo, *J. Chem. Theory Comput.* **2017**, *13*, 6131–6145; c) K. P. Jensen, W. L. Jorgensen, *J. Chem. Theory Comput.* **2006**, *2*, 1499–1509; d) J. N. Canongia Lopes, K. Shimizu, A. A. H. Pádua, Y. Umebayashi, S. Fukuda, K. Fujii, S.-i. Ishiguro, *J. Phys. Chem. B* **2008**, *112*, 9449–9455.
- [3] L. Martinez, R. Andrade, E. G. Birgin, J. M. Martinez, *J. Comput. Chem.* **2009**, *30*, 2157–2164.
- [4] M. Parrinello, A. Rahman, *J. Appl. Phys.* **1981**, *52*, 7182–7190.
- [5] a) W. G. Hoover, *Phys. Rev. A* **1985**, *31*, 1695–1697; b) S. Nose, *Mol. Phys.* **1984**, *52*, 255–268.
- [6] a) M. Neumann, O. Steinhauser, *Chem. Phys. Lett.* **1984**, *106*, 563–569; b) W. L. Jorgensen, D. S. Maxwell, J. Tirado-Rives, *J. Am. Chem. Soc.* **1996**, *118*, 11225–11236.
- [7] a) T. Sigvartsen, J. Songstad, B. Gestblom, E. Noreland, *J. Solution. Chem.* **1991**, *20*, 565–582; b) T. Sigvartsen, B. Gestblom, E. Noreland, J. Songstad, *Acta Chem. Scand.* **1989**, *43*, 103–115.
- [8] M. J. Frisch, G. W. Trucks, H. B. Schlegel, G. E. Scuseria, M. A. Robb, J. R. Cheeseman, G. Scalmani, V. Barone, B. Mennucci, G. A. Petersson, Gaussian Inc., Wallingford, CT **2009**.
- [9] A. D. Becke, *J. Chem. Phys.* **1993**, *98*, 5648–5652.
- [10] A. V. Marenich, C. J. Cramer, D. G. Truhlar, *J. Phys. Chem. B* **2009**, *113*, 6378–6396.
- [11] a) B. H. Besler, K. M. Merz, Jr., P. A. Kollma, *J. Comput. Chem.* **1990**, *11*, 431–439; b) U. C. Singh, P. A. Kollman, *J. Comput. Chem.* **1984**, *5*, 129–145.
- [12] T. Lu, F.-W. Chen, *J. Comput. Chem.* **2012**, *33*, 580–592.
- [13] M. Abadi, A. Agarwal, P. Barham, E. Brevdo, Z. Chen, C. Citro, G. S. Corrado, A. Davis, J. Dean, M. Devin, S. Ghemawat, I. Goodfellow, A. Harp, G. Irving, M. Isard, Y. Jia, R. Jozefowicz, L. Kaiser, M. Kudlur, J. Levenberg, D. Mané, R. Monga, S. Moore, D. Murray, C. Olah, M. Schuster, J. Shlens, B. Steiner, I. Sutskever, K. Talwar, P. Tucker, V. Vanhoucke, F. Vasudevan, F. Viégas, O. Vinyals, P. Warden, M. Wattenberg, M. Wicke, Y. Yu, X. Zheng, **2016**, arXiv preprint arXiv:1603.04467.

Author Contributions

N.Y., X.C., and Q.Z. designed research; N.Y., X.C., X.S., R.Z., Z.-H.F., and X.-X.M. performed research; X.-Q.Z. and B.-Q.L. contributed new reagents/analytic tools; N.Y., X.C., X.S., R.Z., Z.-H.F., X.-X.M., and Q.Z. analyzed data; and N.Y., X.C., and Q.Z. wrote the paper.